

Myeloid Mineralocorticoid Receptor Activation Contributes to Progressive Kidney Disease

Louis L. Huang,^{*†} David J. Nikolic-Paterson,^{*†} Yingjie Han,^{*†} Elyce Ozols,^{*} Frank Y. Ma,^{*†} Morag J. Young,[‡] and Greg H. Tesch^{*†}

^{*}Department of Nephrology and [†]Monash University Department of Medicine, Monash Medical Centre, Clayton, Victoria, Australia, and [‡]Prince Henry's Institute of Medical Research, Clayton, Victoria, Australia

ABSTRACT

Clinical and experimental studies have shown that mineralocorticoid receptor (MR) antagonists substantially reduce kidney injury. However, the specific cellular targets and mechanisms by which MR antagonists protect against kidney injury must be identified. We used conditional gene deletion of MR signaling in myeloid cells (MR^{flox/flox} LysM^{Cre} mice; MyMRKO) or podocytes (MR^{flox/flox} Pod^{Cre} mice; PodMRKO) to establish the role of MR in these cell types in the development of mouse GN. Accelerated anti-glomerular basement membrane GN was examined in groups of mice: MyMRKO, PodMRKO, wild-type (WT) littermates, and WT mice receiving eplerenone (100 mg/kg twice a day; EPL-treated). At day 15 of disease, WT mice had glomerular crescents (37%±5%), severe proteinuria, and a 6-fold increase in serum cystatin-C. MyMRKO, PodMRKO, and EPL-treated mice with GN displayed proteinuria similar to that in these disease controls. However, MyMRKO and EPL-treated groups had a 35% reduction in serum cystatin-C levels and reduced crescent numbers compared with WT mice, whereas PodMRKO mice were not protected. The protection observed in MyMRKO mice appeared to result predominantly from reduced recruitment of macrophages and neutrophils into the inflamed kidney. Suppression of kidney leukocyte accumulation in MyMRKO mice correlated with reductions in gene expression of proinflammatory molecules (TNF- α , inducible nitric oxide synthase, chemokine (C-C motif) ligand 2, matrix metalloproteinase-12), tubular damage, and renal fibrosis and was similar in EPL-treated mice. In conclusion, MR signaling in myeloid cells, but not podocytes, contributes to the progression of renal injury in mouse GN, and myeloid deficiency of MR provides protection similar to eplerenone in this disease.

J Am Soc Nephrol 25: 2231–2240, 2014. doi: 10.1681/ASN.2012111094

Mineralocorticoid receptor (MR) antagonists are known to inhibit renal and cardiovascular disease (CVD) by direct blockade of MR in tissues and by reducing hypertension.¹ They can also suppress kidney damage in animal models of GN and diabetic nephropathy without affecting BP.^{2–6} In addition, MR antagonists provide added protection against proteinuria and loss of renal function when used with standard antihypertensive therapies in patients with diabetic and nondiabetic CKD.^{7–9}

The clinical use of MR antagonists is limited by the development of hyperkalemia due to the importance of the MR in tubular regulation of salt balance.¹⁰ This consequence of MR blockade in the distal tubule is most evident during renal impairment and can require a reduction in the dosage of

MR antagonist or withdrawal of the agent as a therapy.^{7,8} The specific renal cell types that are targeted by MR antagonists to reduce injury during kidney disease have not been clearly identified. Establishing the identity of these cells is an important step toward developing more selective inhibitors of MR signaling that do not interfere with tubular cell function.

Received November 19, 2012. Accepted January 29, 2014.

Published online ahead of print. Publication date available at www.jasn.org.

Correspondence: Dr. Greg Tesch, Department of Nephrology, Monash Medical Centre, 246 Clayton Road, Clayton, VIC 3168, Australia. Email: greg.tesch@monash.edu

Copyright © 2014 by the American Society of Nephrology

Animal studies demonstrate that the protection afforded by MR antagonists in GN and diabetic nephropathy is associated with reductions in renal inflammation, proteinuria, and glomerular injury.^{2,3,5,11} These studies also link MR blockade to suppression of leukocyte recruitment and podocyte injury. This suggests that the major pathologic effects of MR signaling may occur in podocytes and inflammatory cells.

Recent *in vitro* studies have suggested that MR signaling can induce apoptosis in podocytes and oxidative stress in macrophages,^{12,13} which supports a role for MR signaling in these cell types in kidney disease. In addition, an MR deficiency in myeloid cells protects against cardiovascular injury and ischemic cerebral infarcts by reducing inflammation and fibrosis.^{14–16} However, no *in vivo* studies have identified whether MR signaling in podocytes or macrophages is specifically important to the development of kidney disease.

In this study, we created mice with a selective genetic deficiency of MR in myeloid cells or podocytes and used these strains to evaluate the hypothesis that MR signaling in macrophages or podocytes is required for the development of renal injury in a normotensive model of progressive GN.

RESULTS

Mice with Myeloid MR Deficiency Have Normal Leukocyte Levels and Antibody Responses

Analysis of MR^{flox/flox} LysM^{Cre} (MyMRKO) mice found an 80% reduction of MR gene expression in kidney macrophages (Supplemental Table 1) and a 50% reduction in MR protein on blood neutrophils (Supplemental Figure 1). MyMRKO mice had normal circulating levels of white blood cells ($5.2 \pm 0.4 \times 10^9/L$ for wild type [WT] versus $5.0 \pm 0.4 \times 10^9/L$ for MyMRKO) with a similar proportion of monocytes ($1.4\% \pm 1.0\%$ for WT versus $1.3\% \pm 0.9\%$ for MyMRKO) and neutrophils ($9.6\% \pm 0.2\%$ for WT versus $10.9\% \pm 2.0\%$ for MyMRKO). During the development of GN, MyMRKO mice produced a humoral immune response equivalent to that seen in WT mice, which included equal levels of circulating antsheep immunoglobulin and glomerular deposition of mouse immunoglobulin and C3 (Figure 1).

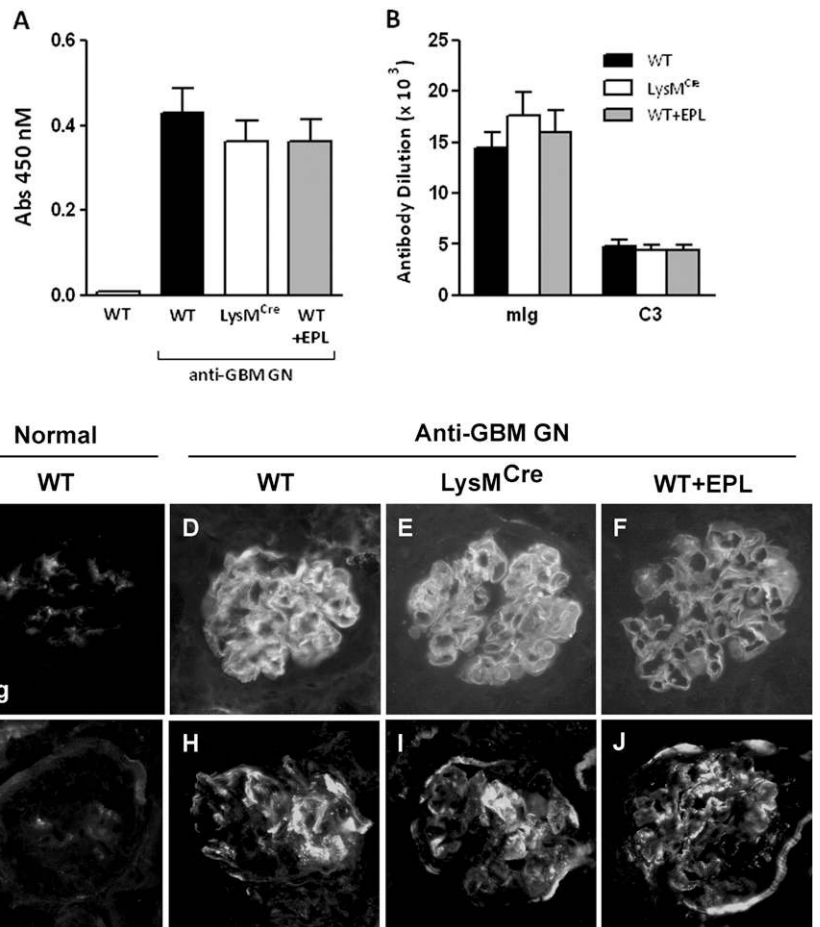


Figure 1. Antibody and complement activity in anti-GBM GN are unaltered by deficiency of MR signaling. (A) Serum levels of mouse anti-sheep immunoglobulin are equivalent in WT, MyMRKO, and eplerenone-treated mice with GN. (B) Antibody titration analysis showed that glomerular deposition of mouse immunoglobulin and C3 are the same in WT, MyMRKO and eplerenone-treated mice with GN. (C–J) Immunofluorescence staining shows extensive glomerular deposition of mouse immunoglobulin and C3 after the development of anti-GBM GN, which was similar in WT, MyMRKO, and eplerenone-treated mice (magnification $\times 400$). Data in A and B are the mean \pm SEM; $n=8$.

Myeloid MR Deficiency Protects Mice from Declining Renal Function in Anti-Glomerular Basement Membrane GN

Pre-experimental analysis showed that urinary protein excretion in MyMRKO mice is equivalent to that in normal mice (Figure 2A). Induction of GN in WT mice resulted in albuminuria at day 1 of disease, which remained elevated at days 7 and 14 (Figure 2A). Administration of eplerenone to WT mice with GN did not affect albuminuria. However, albuminuria was reduced by 40% in MyMRKO compared with WT mice at day 1 of disease but was not different at days 7 or 14 of disease.

Serum levels of cystatin C were similar in WT and MyMRKO mice without disease, indicating that MyMRKO mice had normal renal function (Figure 2B). WT mice had a 6-fold increase in the serum level of cystatin C at day 15 of anti-

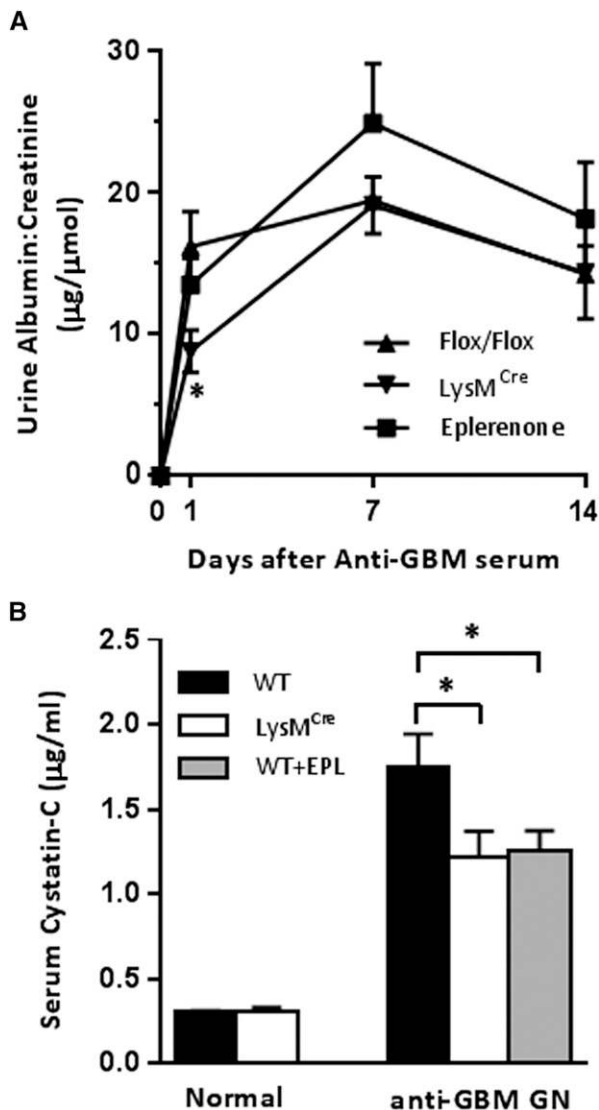


Figure 2. Myeloid MR deficiency protects mice from loss of renal function in anti-GBM GN. (A) Albuminuria was reduced in MyMRKO mice compared with WT and eplerenone-treated mice at day 1 of anti-GBM disease. However, albuminuria was similar in each of these groups at days 7 and 14 of disease. (B) At day 15 of anti-GBM disease, there was a 6-fold increase in serum levels of cystatin C in WT mice, which was reduced by 35% in the MyMRKO and eplerenone-treated groups. Data are the mean \pm SEM; $n=8$. * $P<0.05$ versus WT with disease.

glomerular basement membrane (GBM) GN, which was reduced by approximately 35% in both MyMRKO mice and eplerenone-treated WT mice.

Myeloid MR Deficiency Reduces Kidney Damage in Anti-GBM GN

At day 15 of GN, WT mice had severe histologic kidney damage, which included crescents in 37% of glomeruli (Figure 3, Table 1). In comparison, MyMRKO mice and eplerenone-treated WT mice had significantly reduced crescent formation, with levels

of 26% and 11% of glomeruli, respectively. Immunostaining analysis identified increased glomerular accumulation of myofibroblasts in diseased compared with normal WT mice, which was diminished in MyMRKO and eplerenone-treated WT mice (Figure 3, Table 1).

Extensive damage was also found in the tubulointerstitial area of the renal cortex in mice with GN. Apoptotic cells, identified by immunostaining for activated caspase-3, were mostly located in the tubulointerstitium in diseased WT type mice; however, their numbers were decreased in MyMRKO mice and eplerenone-treated WT mice (Table 1). Similarly, periglomerular and peritubular myofibroblasts were frequently observed in WT mice with GN, and their presence was substantially reduced in MyMRKO mice and eplerenone-treated WT mice (Figure 3, Table 1). Quantitative PCR analysis of whole kidney identified a 30-fold increase in gene expression of COL1A1, FN1, and *PAI-1* in WT mice with GN (Table 1). The expression of these profibrotic genes was about 50% lower in both MyMRKO mice and eplerenone-treated WT mice. In comparison, the elevated levels of TGF- β 1 mRNA seen in the diseased kidneys of WT mice was not reduced in MyMRKO mice or EPL-treated mice with GN (Table 1); however, TGF- β 1 activity was not examined.

Myeloid MR Deficiency Reduces Renal Inflammation in Anti-GBM GN

Because MyMRKO mice showed protection from proteinuria at day 1 of GN, we examined these mice at 3 hours after disease induction to identify whether the early glomerular inflammatory response was affected. Immunostaining demonstrated that neutrophils were scarce in the glomeruli of mice without disease (0.22 ± 0.05 cells/glomerular cross-section [gcs] in WT mice versus 0.21 ± 0.15 cells/gcs in MyMRKO mice). In comparison, there was a marked influx of neutrophils in glomeruli at 3 hours of disease in WT mice (3.5 ± 1.1 cells/gcs), which was reduced by 40% in MyMRKO mice (2.1 ± 0.7 cells/gcs; $P<0.05$) and eplerenone-treated mice (1.9 ± 0.5 cells/gcs; $P<0.05$). At 3 hours of disease, glomerular macrophages were not significantly increased and glomerular CD41⁺ platelets were increased 2-fold but did not differ between WT and MyMRKO strains (data not shown).

At day 15 of GN, neutrophils had diminished to normal levels in the glomeruli of WT mice and were rarely detected in the tubulointerstitium (data not shown). In contrast, the glomerular and interstitial numbers of macrophages and T cells were substantially increased in these mice (Table 2). Compared with the WT mice, MyMRKO mice had a 60%–70% reduction in the accumulation of glomerular and interstitial macrophages at day 15, whereas eplerenone-treated WT mice were less protected from macrophage infiltration (Figure 3, Table 2). At day 15, glomerular T cells were not reduced in MyMRKO mice or by eplerenone treatment; however, the number of interstitial T cells decreased 30% in both these groups (Table 2).

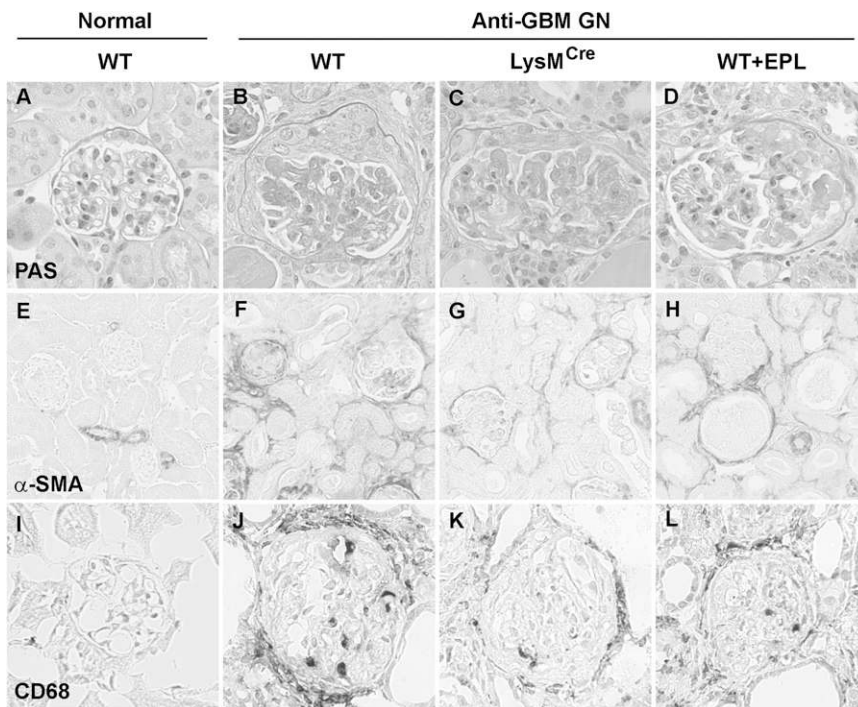


Figure 3. Myeloid MR deficiency reduces kidney damage in anti-GBM GN. Histologic staining with periodic acid–Schiff (PAS) and hematoxylin shows the kidney structure of (A) a normal mouse. In comparison, there is severe damage to glomeruli (crescent formation, sclerosis) and tubules (dilatation, atrophy) in (B) a WT mouse at day 15 of anti-GBM disease, which is attenuated in (C) a MyMRKO mouse and (D) an eplerenone-treated WT mouse. Immunostaining of α -smooth muscle actin was found only in the vasculature in (E) a normal mouse kidney. However, significant expression of α -smooth muscle actin was seen in myofibroblasts accumulating in glomerular, periglomerular, and tubulointerstitial regions in (F) a WT mouse at day 15 of anti-GBM disease, which is reduced in (G) a MyMRKO mouse and (H) an eplerenone-treated WT mouse. Immunostaining identified small numbers of resident CD68⁺ macrophages in (I) a normal mouse kidney. In contrast, there were many infiltrating macrophages in glomeruli and the interstitium of (J) a WT mouse at day 15 of anti-GBM disease, which is reduced in (K) a MyMRKO mouse and (L) an eplerenone-treated WT mouse. Magnification: A–D and I–L, $\times 400$; E–H, $\times 250$.

Table 1. Kidney damage in MyMRKO mice

Analysis	WT	MyMRKO	Anti-GBM GN		
			WT	MyMRKO	WT+EPL
Glomerular crescents (%)	0	0	37 \pm 2	26 \pm 1 ^a	11 \pm 2 ^{a,b}
Apoptotic cells (cells/mm ²)	0.5 \pm 0.2	0.4 \pm 0.2	6.0 \pm 0.5	2.9 \pm 0.2 ^a	3.7 \pm 0.4 ^c
Wilms' tumor-1+podocytes/gcs	10.0 \pm 0.3	9.9 \pm 0.3	3.9 \pm 0.2	3.4 \pm 0.2	4.8 \pm 0.3 ^d
Glomerular myofibroblasts (% area)	0.5 \pm 0.1	0.4 \pm 0.1	12.2 \pm 1.0	4.4 \pm 0.4 ^a	5.6 \pm 0.5 ^a
Interstitial myofibroblasts (% area)	0.4 \pm 0.1	0.2 \pm 0.1	5.3 \pm 0.8	1.2 \pm 0.2 ^a	2.4 \pm 0.5 ^{c,d}
COL1A1 mRNA/18s	1.1 \pm 0.3	2.6 \pm 0.2	38 \pm 4	16 \pm 5 ^c	16 \pm 2 ^a
FN1 mRNA/18s	1.1 \pm 0.2	2.2 \pm 0.2	27 \pm 3	17 \pm 3 ^e	18 \pm 3 ^e
PAI-1 mRNA/18s	1.2 \pm 0.2	2.1 \pm 0.4	35 \pm 11	18 \pm 4	18 \pm 2
TGF- β 1 mRNA/18s	1.2 \pm 0.4	1.3 \pm 0.3	4.4 \pm 0.6	3.7 \pm 0.4	4.9 \pm 0.6

Data are the mean \pm SEM.

^aP<0.001 versus WT with disease.

^bP<0.001 versus MyMRKO with disease.

^cP<0.01 versus WT with disease.

^dP<0.05 versus MyMRKO with disease.

^eP<0.05 versus WT with disease.

PCR analysis of WT diseased kidneys at day 15 identified a marked increase in the gene expression of proinflammatory cytokines (TNF- α , inducible nitric oxide synthase, chemokine [C-C motif] ligand [CCL] 2, matrix metalloproteinase-12 [MMP-12]) associated with a macrophage M1 phenotype, which was reduced in MyMRKO mice and to a lesser extent in the eplerenone group (Table 2). In comparison, gene expression of markers of a M2 macrophage phenotype (arginase-1, CD206) were increased in diseased WT kidneys, but the expression levels were unchanged in MyMRKO mice or by eplerenone treatment. Further PCR analysis found that the gene expression of T cell-related molecules (CD3e, granzyme B, CCL5) were moderately increased in WT kidneys at day 15 of GN; however, only CCL5 expression was reduced in the MyMRKO mice and eplerenone-treated mice (Table 2).

Phenotyping studies were performed on CD11b⁺ macrophages isolated from normal WT kidneys and kidneys obtained from WT or MyMRKO mice at day 15 of GN. PCR analysis found that macrophage expression of CCL2, CCR2, nitric oxide synthase-2, macrophage migration inhibitory factor, and CD163 did not differ between these groups. However, in diseased kidneys some M1 (IL-12, MMP-12) and M2 (arginase-1, CD206, CCR7, IL-10, heme oxygenase-1) markers significantly increased and TNF- α and some oxidative stress markers (Cyba/p22phox, Cybb/Nox2) decreased; these changes were not different between WT and MyMRKO mice (Supplemental Table 1).

Myeloid MR Deficiency Does Not Affect Tubular Regulation of Salt Balance

Analysis of serum K⁺ levels found no evidence of hyperkalemia in MyMRKO mice or in mice treated with eplerenone (Figure 4A). However, when we assessed urine levels of Na⁺ and K⁺, we found that eplerenone treatment significantly increased Na⁺/K⁺ in urine, whereas urine Na⁺/K⁺ remained similar in WT and MyMRKO mice with and without GN (Figure 4B).

Mice with MR Deficiency in Podocytes Have Normal Kidney Development

Deletion of MR in podocytes in MR^{flox/flox} Pod^{cre/-} (PodMRKO) mice was confirmed

Table 2. Kidney inflammation in MyMRKO mice

Analysis	WT	MyMRKO	Anti-GBM GN		
			WT	MyMRKO	WT+EPL
Glomerular CD68 (cells/gcs)	0.15±0.01	0.22±0.04	2.0±0.1	0.9±0.1 ^a	1.4±0.1 ^{b,c}
Glomerular CD3 (cells/gcs)	0.4±0.1	0.4±0.1	1.4±0.1	1.2±0.1	1.2±0.1
Glomerular Ly6G (cells/gcs)	0.09±0.03	0.17±0.05	0.12±0.02	0.10±0.01	0.17±0.07
Interstitial CD68 (% area)	0.7±0.1	0.7±0.1	5.2±0.6	2.1±0.2 ^a	4.4±0.6 ^d
Interstitial CD3 (cells/mm ²)	7±1	8±2	150±10	103±11 ^b	103±13 ^e
TNF- α mRNA/18s	1.2±0.2	1.0±0.2	10.1±1.3	4.1±1.0 ^b	9.0±1.2
NOS2 mRNA/18s	1.1±0.2	0.7±0.1	3.4±0.5	1.3±0.3 ^b	1.6±0.2 ^b
CCL2 mRNA/18s	1.3±0.4	1.6±0.6	10.0±1.6	4.0±1.4 ^e	7.2±1.3
MMP12 mRNA/18s	1.1±0.2	0.6±0.1	26±5	7.7±3.1 ^b	7.9±1.5 ^b
Arginase-1 mRNA/18s	1.3±0.3	1.0±0.3	33±7	25±10	40±14
CD206 mRNA/18s	1.2±0.3	0.9±0.2	58±11	32±10	35±5
CD3e mRNA/18s	1.2±0.4	1.7±0.6	4.2±0.7	2.6±1.0	2.1±0.8
IL-12 β mRNA/18s	0.8±0.1	1.0±0.2	4.9±1.9	4.0±1.4	3.5±1.3
Granzyme B mRNA/18s	1.1±0.3	0.6±0.1	3.6±0.6	2.8±1.3	3.0±0.6
CCL5 mRNA/18s	1.0±0.1	0.7±0.1	2.9±0.4	1.3±0.4 ^b	1.2±0.3 ^b

Data are the mean±SEM. NOS2, nitric oxide synthase-2.

^aP<0.001 versus WT with disease.

^bP<0.01 versus WT with disease.

^cP<0.05 versus MyMRKO with disease.

^dP<0.01 versus MyMRKO with disease.

^eP<0.05 versus WT with disease.

by immunostaining in kidney sections and by a 50% reduction in MR gene expression in isolated glomeruli (Figure 5). MR immunostaining was readily detected in the distal nephron and in podocytes of WT mice but was absent in the podocytes of PodMRKO mice (Figure 5, Supplemental Figure 2). Additional immunohistochemistry analysis showed that PodMRKO mice had the same number of WT1+podocytes (10.0±0.7 cells/gcs) as normal WT mice (10.0±0.7 cells/gcs) and that their kidney structure was normal (not shown).

Podocyte MR Deficiency Does Not Prevent Loss of Renal Function in Anti-GBM GN

Urine protein excretion and renal function were identical in WT and PodMRKO mice without disease (Figure 6). Induction of GN resulted in the development of proteinuria in WT and PodMRKO mice that was equivalent at days 1, 7, and 14 (Figure 6A). Similarly, both WT and PodMRKO mice had a 6-fold increase in the serum levels of cystatin C at day 15 of GN, indicating that these strains had equal loss of renal function (Figure 6B).

Podocyte MR Deficiency Does Not Prevent Renal Damage in Anti-GBM GN

Periodic acid–Schiff staining showed that the severity of kidney damage in PodMRKO mice was similar to that in WT mice at day 15 of GN (Figure 7). PodMRKO mice with GN had a high proportion of glomeruli with crescents, which was not different than findings in WT mice (Table 3). Immunostaining of WT-1 revealed that podocyte numbers were similarly reduced in WT mice and PodMRKO mice at day 15 of GN compared with mice without disease (Table 3). In addition,

immunostaining demonstrated that the kidney accumulation of myofibroblasts and apoptotic cells were equivalent in WT mice and PodMRKO mice with GN (Table 3).

DISCUSSION

Our study has demonstrated a pathologic role for MR signaling in myeloid cells, but not podocytes, in a model of rapidly progressive GN. To our knowledge, this is the first report that *in vivo* targeting of MR signaling in myeloid cells can reduce renal injury. Furthermore, we have shown that blockade of MR signaling in myeloid cells can achieve a level of renal protection similar to that of systemic MR blockade with eplerenone.

MR signaling played a role in the initial immune response in anti-GBM GN. In this model, the rapid glomerular influx of neutrophils at 3 hours of disease was reduced by 40% in both MyMRKO mice and

WT mice treated with eplerenone. Notably, MyMRKO mice showed a similar reduction in proteinuria at day 1; however, this protection was not seen with eplerenone treatment, suggesting that a more thorough inhibition of MR in myeloid cells is required for this effect. Previous research has demonstrated that a transient infiltration of neutrophils at the onset of anti-GBM disease is responsible for the induction of glomerular inflammation and proteinuria but not the progression of injury.¹⁷ In addition, glomerular macrophages did not increase at this stage of disease. Therefore, our findings suggest that MR signaling in neutrophils may contribute to early glomerular damage and the induction of proteinuria in this model, which could involve effects on neutrophil activation and subsequent injury to podocytes, glomerular endothelial cells, and tubular cells.

At day 15 of GN, when a neutrophil infiltrate was absent, deficiency of MR signaling was associated with suppression of the macrophage-dependent inflammatory response. Compared with findings in WT mice, glomerular and interstitial macrophages and gene expression of macrophage-related proinflammatory cytokines were markedly reduced in MyMRKO mice and to a similar or lesser extent in eplerenone-treated WT mice. In contrast, T-cell accumulation and activity appeared less affected by deficiency of MR signaling. In anti-GBM disease, MyMRKO and EPL-treated mice had reduced kidney gene expression of the T-cell chemokine CCL5, but the levels of other T cell–related genes (CD3e, IL-12 β , and granzyme B) remained similar to levels in WT mice. In addition, our study found that myeloid MR deficiency had no effect on antibody responses, indicating that antigen presentation was not altered. These findings suggest that the effect

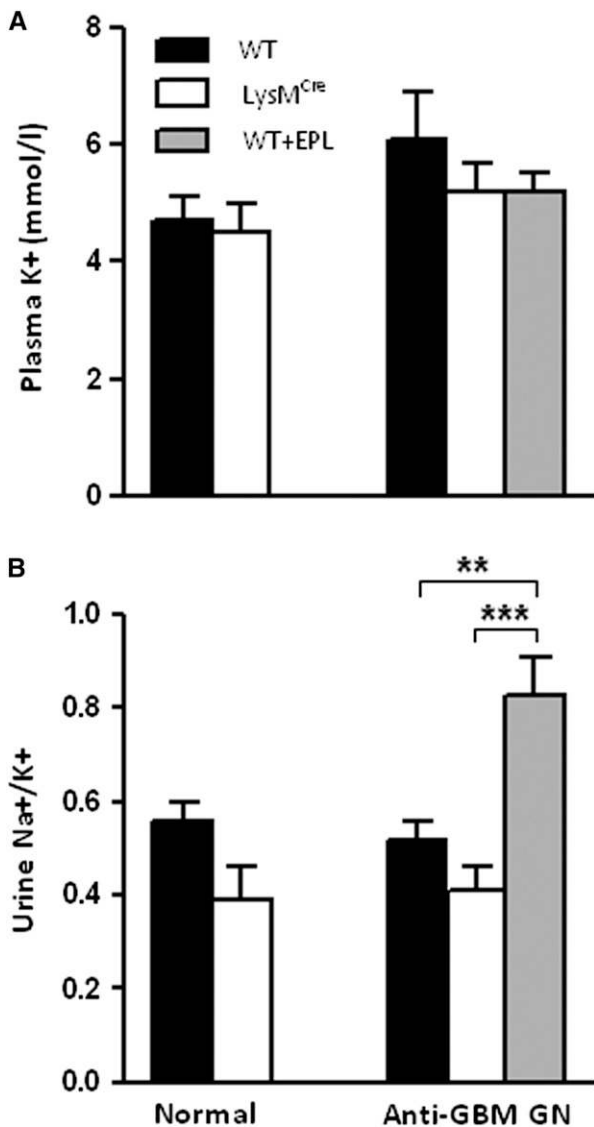


Figure 4. Myeloid MR deficiency does not alter salt balance. (A) Plasma levels of K⁺ were similar in mice with and without anti-GBM GN and were not affected by myeloid MR deficiency or eplerenone treatment. (B) Urine levels of Na⁺/K⁺ were equivalent in WT and MyMRKO mice with and without disease. In contrast, urine Na⁺/K⁺ was significantly elevated in eplerenone-treated WT mice, indicating that tubular regulation of salt balance had been affected. Data are the mean±SEM; n=8; **P<0.01; ***P<0.001.

of MR blockade on inflammation during the progression of anti-GBM GN is primarily through macrophage MR signaling.

Myeloid MR deficiency and EPL treatment had specific anti-inflammatory effects in anti-GBM GN, the most prominent being a suppression of macrophage recruitment during disease progression. This is consistent with previous findings showing that eplerenone reduces kidney expression of leukocyte adhesion molecules.¹⁸ Furthermore, MyMRKO mice had reduced gene expression of proinflammatory cytokines associated with the reduced macrophage infiltrate. In comparison,

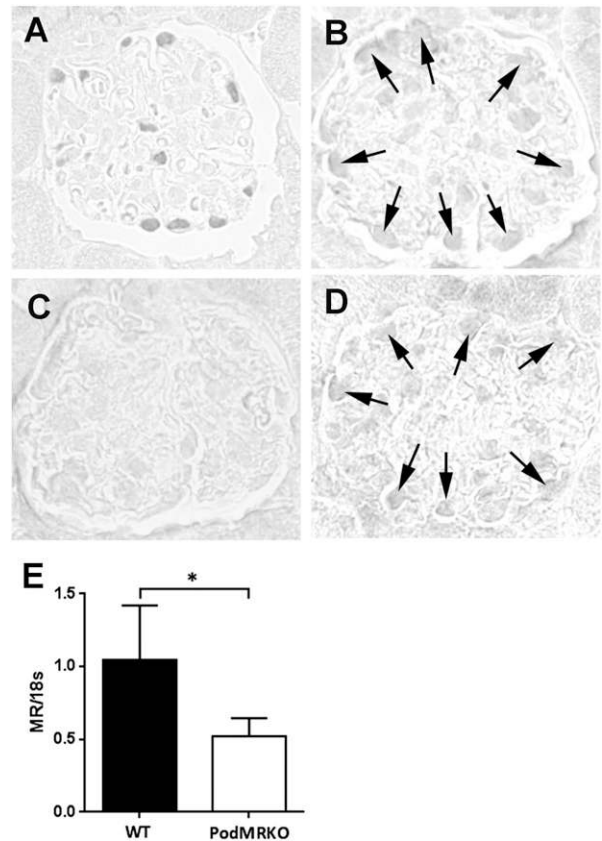


Figure 5. MR expression by podocytes is absent in PodMRKO mice. (A) Immunostaining of Cre-recombinase in the podocytes of a MR^{fl^{ox}/fl^{ox}}/Podocin^{Cre^{-/-}} (PodMRKO) mouse. Immunostaining of serial sections shows that PodMRKO mice have (B) normal glomerular expression of the podocyte marker WT1 (arrows) and that their podocytes are (C) deficient in MR expression. In contrast, MR immunostaining is observed in (D) the podocytes of a WT mouse (arrows). Graph (E) shows that MR gene expression is reduced by 50% in the glomeruli of PodMRKO compared with WT mice. Magnification: A–D, ×400. *P<0.05.

studies in models of CVD and cerebral ischemia have shown that MyMRKO mice have reduced levels of M1 cytokines and that this can occur with and without a reduction in macrophage numbers.^{15,16,19} Notably, some of these *in vivo* studies and experiments using cultured cells have indicated that a deficiency of MR signaling in macrophages can alter macrophage gene expression toward an M2 alternatively activated phenotype.^{15,16} Our PCR analysis of CD11b⁺ macrophages isolated from WT and MyMRKO kidneys at day 15 of disease found no difference in the M1/M2 phenotype. Thus, the difference in expression of most of these markers in the diseased kidneys is probably due to changes in macrophage numbers rather than in their phenotype. In addition, macrophages from diseased kidneys showed a significant increase in mRNA levels of some M1 (IL-12, MMP-12) and M2 (arginase-1, CD206, CCR7, IL-10, heme oxygenase-1) markers and a decrease in TNF-α compared with macrophages from normal kidneys. This mixed

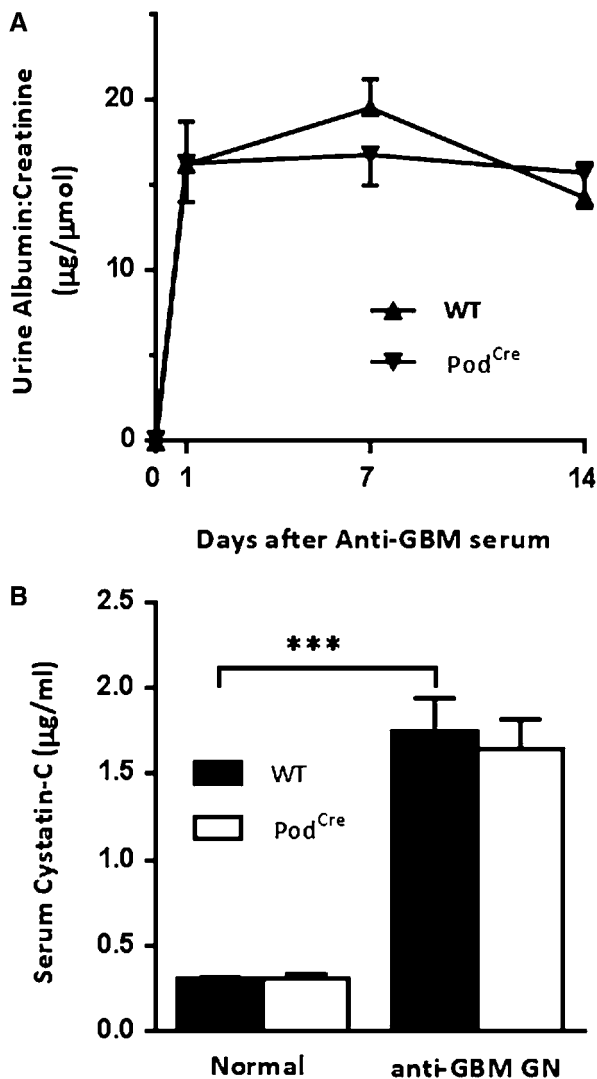


Figure 6. Podocyte MR deficiency does not prevent loss of renal function in anti-GBM GN. (A) Albuminuria was equivalent in PodMRKO mice compared with WT mice at days 1, 7, and 14 of anti-GBM disease. (B) At day 15 of anti-GBM disease, the serum levels of cystatin C were equally elevated in PodMRKO and WT mice, indicating a similar decline in renal function. Data are the mean \pm SEM; $n=8$; *** $P<0.001$.

macrophage phenotype is consistent with our recent analysis of rat anti-GBM disease, which showed a transition from an M1 phenotype during acute inflammation to a more M2 phenotype during the fibrotic phase.²⁰ However, these findings do not rule out the possibility that MR deficiency may affect the kidney macrophage phenotype at an earlier stage of disease. Aldosterone infusion into mice induces oxidative stress in macrophages.¹³ Therefore, MyMRKO mice may be protected from kidney oxidative stress early in disease when macrophage MR signaling may be at a peak in WT mice. Furthermore, it is also possible that deletion of MR occurs in some dendritic cells in MyMRKO mice, which may contribute to protection against anti-GBM GN.

Kidney damage in anti-GBM GN was markedly reduced by myeloid MR deficiency. Glomerular crescents, myofibroblast accumulation, and gene expression of profibrotic molecules (COL1A1, FN1, *PAI-1*) were all decreased in MyMRKO mice compared with WT mice. This suppression of profibrotic molecule gene expression indicates a reduction in TGF- β 1 activity, although TGF- β 1 mRNA levels were not affected by MR deficiency/blockade. Eplerenone-treated mice had a similar reduction in myofibroblasts and matrix gene expression but a greater reduction in crescents than MyMRKO mice. This indicates that eplerenone has additional antiproliferative or antifibrotic effects on parietal epithelial cells to those caused by blockade of myeloid MR. We also found that MyMRKO mice and eplerenone-treated mice were equally protected against declining renal function, suggesting that macrophage MR signaling is responsible for the injury-dependent loss of renal function in this model. These findings are similar to those reported in studies in CVD, which show that systemic MR blockade can reduce histologic lesions and fibrosis in the absence of an effect on hypertension.²¹

Normal regulation of salt balance appears to be unaffected by myeloid MR deficiency. In our study, hyperkalemia was not detected in the serum of MyMRKO or eplerenone-treated mice. However, urine levels of Na^+/K^+ were increased in eplerenone-treated mice, but not in MyMRKO mice, suggesting that systemic MR blockade was causing tubular dysfunction.²² Therefore, selective blockade of MR signaling in macrophages has potential for treating kidney and cardiovascular disease, without disturbing salt regulation by tubules.

In contrast to MyMRKO mice, PodMRKO mice had no protection against renal injury in anti-GBM GN. WT and PodMRKO mice had equivalent albuminuria and loss of renal function during the progression of disease. Glomerular and tubulointerstitial damage was also similar in both strains. This indicates that MR signaling in podocytes is not required for the progression of anti-GBM GN. Previous studies have identified that aldosterone can induce MR-mediated podocyte injury in cultured cells²³ and when infused into uninephrectomized rats on a high-salt diet.²⁴ Furthermore, systemic MR blockade reduces podocyte loss or damage in diabetic rats.^{11,12} Therefore, our data showing a lack of prevention of albuminuria in diseased mice with systemic MR blockade or podocyte MR deficiency indicates that podocyte damage in this rapidly progressive GN model is mediated by injury mechanisms that are independent of MR. However, the ability of MR antagonists to reduce proteinuria in CKD, suggests that podocyte MR signaling may play a role in chronic proteinuria.

In conclusion, our study has identified that myeloid MR deficiency protects against development of GN. This was primarily due to inhibition of the transient neutrophil influx during disease induction and the inhibition of kidney macrophage accumulation during disease progression. These findings suggest that MR blockade could be targeted to myeloid cells, or more specifically macrophages, to avoid the deleterious consequences of systemic MR antagonism on tubular regulation of salt balance. However,

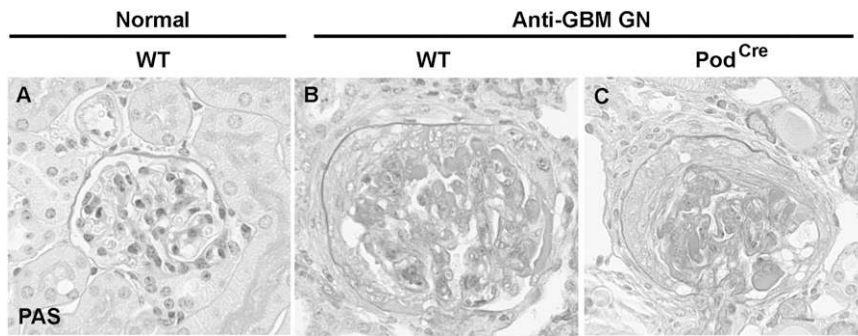


Figure 7. Podocyte MR deficiency does not protect against kidney damage in anti-GBM GN. Histologic staining with periodic acid–Schiff (PAS) and hematoxylin shows the kidney structure of (A) a normal mouse. In comparison, there is severe damage to glomeruli (crescent formation, sclerosis) and tubules (dilatation, atrophy) in (B) a WT mouse at day 15 of anti-GBM disease, which is similar in (C) a PodMRKO mouse. Magnification, $\times 400$.

Table 3. Kidney damage in PodMRKO mice

Analysis	WT	PodMRKO	Anti-GBM GN	
			WT	PodMRKO
Glomerular crescents (%)	0	0	37 \pm 2	37 \pm 5
Wilms' tumor-1+podocytes/gcs	10.0 \pm 0.3	10.0 \pm 0.3	3.9 \pm 0.2	4.3 \pm 0.2
Apoptotic cells (cells/mm ²)	0.5 \pm 0.2	0.5 \pm 0.2	6.0 \pm 0.5	5.1 \pm 0.6
Glomerular myofibroblasts (% area)	0.5 \pm 0.1	0.5 \pm 0.1	12.5 \pm 1.0	11.6 \pm 1.2
Interstitial myofibroblasts (% area)	0.4 \pm 0.1	0.4 \pm 0.1	5.3 \pm 0.8	6.8 \pm 0.8

Data are the mean \pm SEM.

further testing is required to establish the role of macrophage MR signaling in chronic forms of kidney disease, such as diabetic nephropathy.

CONCISE METHODS

Animal Model

Conditional gene deletion of MR was performed in C57BL/6 mice using the CreLoxP system. Mice with homozygous floxed MR gene were crossed with littermates expressing Cre recombinase under the control of a lysozyme M promoter,¹⁴ to create MR^{flox/flox} LysM^{cre/-} (MyMRKO) mice lacking MR in mature myeloid cells (neutrophils, macrophages), or a podocin promoter,²⁵ to create MR^{flox/flox} Pod^{cre/-} (PodMRKO) mice lacking MR in podocytes. MR^{flox/flox} littermates were used as WT controls. The genotyping details are presented in Supplemental Table 2.

For experimentation, 12-week-old female mice ($n=8$) were pre-immunized subcutaneously with 1 mg sheep IgG in Freund complete adjuvant. Four days later, GN was induced by intravenous injection of sheep anti-mouse GBM serum (10 μ l/g). Groups were euthanized after 3 hours of disease (to examine the initial inflammatory response) or after 15 days of disease (to examine the progression of renal damage). To compare conditional MR gene deletion with systemic MR blockade, groups of diseased WT mice were given

eplerenone (100 mg/kg twice daily) by gavage, beginning 2 hours before disease induction. All animal experiments were performed in accordance with the guidelines of the Monash Medical Centre Animal Ethics Committee.

Hematology and Biochemical Analysis

Urine was collected from mice housed in metabolic cages. At day 15, heparinized blood and serum were collected from anesthetized mice. White blood cell counts were determined by a hematology analyzer (Cell-Dyn 3700; Abbott Laboratories, North Chicago, IL). Urine creatinine levels were determined by the Jaffe rate reaction method. ELISAs were used to measure urine levels of albumin (Bethyl Laboratories, Montgomery, TX) and serum levels of cystatin C (BioVendor, Karasek, Czech Republic) and immunoglobulin.²⁶ Levels of K⁺ or Na⁺ in plasma or urine were determined by indirect potentiometry using ion selective electrodes.

Antibodies

Antibodies used in this study were anti-MR (2B6, a gift from Professor Celso Gomez-Sanchez, University of Mississippi), anti-CD68 (FA-11; Serotec, Oxford, UK), anti-Ly6g (Abcam, Inc., Cambridge, UK), anti-CD3 (KT3; Abcam, Inc.), anti-CD41 (Serotec), anti- α -smooth muscle actin (1A4; Sigma-Aldrich, St. Louis, MO), anti-cleaved caspase 3 (Cell Signaling Technology, Beverly, MA), anti-Wilms' tumor antigen 1 (Santa Cruz Biotechnology, Santa Cruz, CA), anti-Cre (Novagen, Madison, WI), fluorescein-conjugated anti-CD11b (BD Biosciences, San Jose, CA), fluorescein conjugated sheep F(ab)2 fragment to mouse immunoglobulin (Silenus, Melbourne, Australia), and fluorescein conjugated goat F(ab)2 fragment to mouse C3 (MP Biomedicals, Solon, OH).

Isolation of Kidney Macrophages

Kidneys were decapsulated, diced, and incubated with 1 mg/ml collagenase (Sigma-Aldrich) and 0.1 mg/ml DNase I (Invitrogen, Carlsbad, CA) in DMEM at 37°C for 30 minutes with shaking. Following erythrocyte lysis, the cells were filtered (70 μ m) and incubated with fluorescein-conjugated CD11b antibody for 30 minutes at 4°C before FACS (MoFlo XDP cell sorter; Beckman Coulter, Brea, CA). Approximately 1.5–2.5 \times 10⁶ CD11b⁺/propidium iodide cells were isolated from two pooled diseased kidneys or four pooled normal kidneys.

Real-Time PCR

Total RNA was extracted from whole kidney, magnetic-bead isolated glomeruli,²⁷ or isolated kidney macrophages using Trizol (Invitrogen) and reverse transcribed with random primers using the SuperScript First-Strand Synthesis kit (Invitrogen). Real-time PCR analysis was performed as previously described.²⁸ The Taqman probe and primer sequences are listed in Supplemental Table 3.

Histology and Immunostaining

Formalin-fixed kidney sections (2 μm) were stained with periodic acid-Schiff reagent to identify kidney structure and crescent formation, and with hematoxylin to distinguish cell nuclei. The percentage of glomeruli with crescents was assessed by microscopy.

Immunostaining procedures are detailed in the Supplemental Methods. Briefly, immunofluorescence staining of glomerular immunoglobulin and C3 was performed on ethanol-fixed sections and scored as previously described.²⁶ Immunoperoxidase staining for leukocytes (CD68, CD3, Ly6g) was performed on 2% paraformaldehyde-lysine-periodate-fixed kidney cryostat sections and assessed using established protocols.²⁸ Immunoperoxidase staining for MR, α -smooth muscle actin, activated caspase-3, and Wilms' tumor-1 was performed on formalin-fixed sections (4 μm) and analyzed according to a previous report.²⁸ All scoring was performed on blinded slides.

Statistical Analyses

Statistical differences between two groups were analyzed by *t* test, and differences between multiple groups were assessed by ANOVA with *post hoc* analysis using Tukey multiple comparison test. Data were analyzed using GraphPad Prism 5.0 (GraphPad Software, San Diego, CA) and was recorded as the mean \pm SEM, with $P < 0.05$ defined as indicating a statistically significant difference.

ACKNOWLEDGMENTS

We thank Professor Susan Quaggin (Samuel Lunenfeld Research Institute, Mount Sinai Hospital, Toronto, ON, Canada) for providing Podocin^{Cre} mice and Julie Ho for her technical support. This work was supported by the Victorian Government's Operational Infrastructure Support Program, a grant from Prince Henry's Institute of Medical Research, and a scholarship from the National Health and Medical Research Council of Australia (L.H.).

DISCLOSURES

None.

REFERENCES

- Shibata H, Itoh H: Mineralocorticoid receptor-associated hypertension and its organ damage: Clinical relevance for resistant hypertension. *Am J Hypertens* 25: 514–523, 2012
- Zitt E, Eller K, Huber JM, Kirsch AH, Tagwerker A, Mayer G, Rosenkranz AR: The selective mineralocorticoid receptor antagonist eplerenone is protective in mild anti-GBM glomerulonephritis. *Int J Clin Exp Pathol* 4: 606–615, 2011
- Qin D, Morita H, Inui K, Tayama H, Inoue Y, Yoshimura A: Aldosterone mediates glomerular inflammation in experimental mesangial proliferative glomerulonephritis. *J Nephrol* 26: 199–206, 2012.
- Lian M, Hewitson TD, Wigg B, Samuel CS, Chow F, Becker GJ: Long-term mineralocorticoid receptor blockade ameliorates progression of experimental diabetic renal disease. *Nephrol Dial Transplant* 27: 906–912, 2012
- Han SY, Kim CH, Kim HS, Jee YH, Song HK, Lee MH, Han KH, Kim HK, Kang YS, Han JY, Kim YS, Cha DR: Spironolactone prevents diabetic nephropathy through an anti-inflammatory mechanism in type 2 diabetic rats. *J Am Soc Nephrol* 17: 1362–1372, 2006
- Guo C, Martinez-Vasquez D, Mendez GP, Toniolo MF, Yao TM, Oestreicher EM, Kikuchi T, Lapointe N, Pojoga L, Williams GH, Ricchiuti V, Adler GK: Mineralocorticoid receptor antagonist reduces renal injury in rodent models of types 1 and 2 diabetes mellitus. *Endocrinology* 147: 5363–5373, 2006
- Rossing K, Schjoedt KJ, Smidt UM, Boomsma F, Parving H-H: Beneficial effects of adding spironolactone to recommended antihypertensive treatment in diabetic nephropathy: A randomized, double-masked, cross-over study. *Diabetes Care* 28: 2106–2112, 2005
- van den Meiracker AH, Baggen RG, Pauli S, Lindemans A, Vulto AG, Poldermans D, Boomsma F: Spironolactone in type 2 diabetic nephropathy: Effects on proteinuria, blood pressure and renal function. *J Hypertens* 24: 2285–2292, 2006
- Boesby L, Elung-Jensen T, Klausen TW, Strandgaard S, Kamper AL: Moderate antiproteinuric effect of add-on aldosterone blockade with eplerenone in non-diabetic chronic kidney disease. A randomized cross-over study. *PLoS ONE* 6: e26904, 2011
- Fuller PJ, Young MJ: Mechanisms of mineralocorticoid action. *Hypertension* 46: 1227–1235, 2005
- Nishiyama A, Kobori H, Konishi Y, Morikawa T, Maeda I, Okumura M, Kishida M, Hamada M, Nagai Y, Nakagawa T, Ohashi N, Nakano D, Hitomi H, Imanishi M: Mineralocorticoid receptor blockade enhances the antiproteinuric effect of an angiotensin II blocker through inhibiting podocyte injury in type 2 diabetic rats. *J Pharmacol Exp Ther* 332: 1072–1080, 2010
- Lee SH, Yoo TH, Nam BY, Kim DK, Li JJ, Jung DS, Kwak SJ, Ryu DR, Han SH, Lee JE, Moon SJ, Han DS, Kang SW: Activation of local aldosterone system within podocytes is involved in apoptosis under diabetic conditions. *Am J Physiol Renal Physiol* 297: F1381–F1390, 2009
- Keidar S, Kaplan M, Pavlotzky E, Coleman R, Hayek T, Hamoud S, Aviram M: Aldosterone administration to mice stimulates macrophage NADPH oxidase and increases atherosclerosis development: A possible role for angiotensin-converting enzyme and the receptors for angiotensin II and aldosterone. *Circulation* 109: 2213–2220, 2004
- Rickard AJ, Morgan J, Tesch G, Funder JW, Fuller PJ, Young MJ: Deletion of mineralocorticoid receptors from macrophages protects against deoxycorticosterone/salt-induced cardiac fibrosis and increased blood pressure. *Hypertension* 54: 537–543, 2009
- Usher MG, Duan SZ, Ivaschenko CY, Frieler RA, Berger S, Schütz G, Lumeng CN, Mortensen RM: Myeloid mineralocorticoid receptor controls macrophage polarization and cardiovascular hypertrophy and remodeling in mice. *J Clin Invest* 120: 3350–3364, 2010
- Frieler RA, Meng H, Duan SZ, Berger S, Schütz G, He Y, Xi G, Wang MM, Mortensen RM: Myeloid-specific deletion of the mineralocorticoid receptor reduces infarct volume and alters inflammation during cerebral ischemia. *Stroke* 42: 179–185, 2011
- Takazoe K, Tesch GH, Hill PA, Hurst LA, Jun Z, Lan HY, Atkins RC, Nikolic-Paterson DJ: CD44-mediated neutrophil apoptosis in the rat. *Kidney Int* 58: 1920–1930, 2000
- Kobayashi N, Hara K, Tojo A, Onozato ML, Honda T, Yoshida K, Mita S, Nakano S, Tsubokou Y, Matsuoka H: Eplerenone shows renoprotective effect by reducing LOX-1-mediated adhesion molecule, PKCepsilon-MAPK-p90RSK, and Rho-kinase pathway. *Hypertension* 45: 538–544, 2005
- Bienvenu LA, Morgan J, Rickard AJ, Tesch GH, Cranston GA, Fletcher EK, Delbridge LM, Young MJ: Macrophage mineralocorticoid receptor signaling plays a key role in aldosterone-independent cardiac fibrosis. *Endocrinology* 153: 3416–3425, 2012
- Han Y, Ma FY, Tesch GH, Manthey CL, Nikolic-Paterson DJ: Role of macrophages in the fibrotic phase of rat crescentic glomerulonephritis. *Am J Physiol Renal Physiol* 304: F1043–F1053, 2013
- Tsukamoto O, Minamino T, Sanada S, Okada K, Hirata A, Fujita M, Shintani Y, Yulin L, Asano Y, Takashima S, Yamasaki S, Tomoike H, Hori

- M, Kitakaze M: The antagonism of aldosterone receptor prevents the development of hypertensive heart failure induced by chronic inhibition of nitric oxide synthesis in rats. *Cardiovasc Drugs Ther* 20: 93–102, 2006
22. Eudy RJ, Sahasrabudhe V, Sweeney K, Tugnait M, King-Ahmad A, Near K, Loria P, Banker ME, Piotrowski DW, Boustany-Kari CM: The use of plasma aldosterone and urinary sodium to potassium ratio as translatable quantitative biomarkers of mineralocorticoid receptor antagonism. *J Transl Med* 9: 180, 2011
23. Chen C, Liang W, Jia J, van Goor H, Singhal PC, Ding G: Aldosterone induces apoptosis in rat podocytes: Role of PI3-K/Akt and p38MAPK signaling pathways. *Nephron, Exp Nephrol* 113: e26–e34, 2009
24. Shibata S, Nagase M, Yoshida S, Kawachi H, Fujita T: Podocyte as the target for aldosterone: roles of oxidative stress and Sgk1. *Hypertension* 49: 355–364, 2007
25. Moeller MJ, Sanden SK, Soofi A, Wiggins RC, Holzman LB: Podocyte-specific expression of cre recombinase in transgenic mice. *Genesis* 35: 39–42, 2003.
26. Tesch GH, Hill PA, Wei M, Nikolic-Paterson DJ, Dutartre P, Atkins RC: LF15-0195 prevents the induction and inhibits the progression of rat anti-GBM disease. *Kidney Int* 60: 1354–1365, 2001
27. Takemoto M, Asker N, Gerhardt H, Lundkvist A, Johansson BR, Saito Y, Betsholtz C: A new method for large scale isolation of kidney glomeruli from mice. *Am J Pathol* 161: 799–805, 2002
28. Lim AK, Ma FY, Nikolic-Paterson DJ, Kitching AR, Thomas MC, Tesch GH: Lymphocytes promote albuminuria, but not renal dysfunction or histological damage in a mouse model of diabetic renal injury. *Diabetologia* 53: 1772–1782, 2010

This article contains supplemental material online at <http://jasn.asnjournals.org/lookup/suppl/doi:10.1681/ASN.2012111094/-/DCSupplemental>.